JOURNAL OF GEOPHYSICAL RESEARCH, VOL. 96, NO. A4, PAGES 5437–5445, APRIL 1, 1991

MODELING THE EFFECTS OF FAST SHOCKS ON SOLAR WIND MINOR IONS

Xuepu Zhao

Center for Space Science and Astrophysics, Stanford University, Stanford, California.

K. W. Ogilvie

Laboratory for Extraterrestrial Physics, NASA Goddard Space Flight Center
Greenbelt, Maryland

Y. C. Whang

Department of Mechanical Engineering, Catholic University of America, Washington, D. C.

Abstract. Observations show that when α particles and other minor ions in the solar wind plasma encounter fast shocks they are heated more than protons and their bulk motion is decelerated less than protons. These effects have been studied using a three-fluid model, and the model predictions have been compared with observations. The comparison indicates that for supercritical fast shocks the three-fluid model can explain cross-shock minor ion heating which is significantly greater than that of protons. When the ratio of specific heats for minor ions, γ_α, equals 2, both the lesser cross-shock deceleration and the greater heating of minor ions than of protons can be predicted by the model; thus the minor ion heating through the shock transition region is consistent with the involvement of 2 degrees of freedom. Because the analysis is formulated in the de Hoffmann-Teller frame of reference, the method is not valid for perpendicular shocks or when the angle is large. These results agree with the few extant observations and might be confirmed by further observations at the Earth's bow shock.

1. Introduction

It has long been recognized that minor ions in the solar wind have temperature roughly proportional to ion masses and have velocities close to the proton velocity [Neugebauer, 1981; Ogilvie et al., 1980; Schmidt et al., 1980]. Since the beginning of the 1980s, although there have been few studies of minor ions, some effects of interplanetary traveling shocks on the solar wind minor ions have been measured. The ISEE 3 spacecraft first found that at six strong interplanetary traveling shocks the decrease in velocity of α particle flow across the shock was less than that for protons, and at four other shocks their changes are approximately identical [Ogilvie et al., 1982; K. W. Ogilvie, private communication, 1989]. The Prognoz 8 spacecraft crossed nine interplanetary shocks and observed the same phenomena; more specifically, its observational results suggested that for shocks with density ratio (downstream to upstream) greater than 2 the velocity change ratio of α particles to protons is less than unity, and for shocks with density ratio less than 2 the velocity change ratio close to 1. The spacecraft also observed cross-shock heating of the α particles greater than that of protons [Zastenker and Borodkova, 1984]. By using 20 traveling shocks observed at 1 AU by Prognoz 7 and Prognoz 8, the results of superposed epoch analysis suggested that α particle heating at the shock is greater by 5–7 times than that of protons, with the upstream temperature ratio of α particles to protons being about 4 (N. L. Borodkova, private communication, 1989). No systematic studies of minor ions at the bow shock have been made, but some effects on minor ions have been observed across the bow shock [Neugebauer, 1970; Peterson et al., 1979]. Recent analysis of Prognoz 10 observations suggests that deflection of the solar wind ion flux takes place earlier than heating of ions, the deflection of protons and that of α particles near the shock front are different, and the reflection of α particles is very small [Zastenker et al., 1987]. The AMPTE Charge Composition Explorer recently observed shell-like He^{2+} and O^{6+} velocity distribution functions on the downstream side of the Earth's bow shock. The distributions are centered on the downstream H^+ bulk velocity and have radii proportional to mass per charge. These quasi-perpendicular bow shock observations are consistent with mass per charge dependent processes influenced by the electrostatic cross-shock potential. The increased α particle bulk velocity over that of protons in the shock rest frame was interpreted as being due to incomplete scattering of the He^{2+} shell distribution on the downstream region. The existence of a "shoulder" of He^{2+} ions may indicate the presence of reflecting, gyrating He^{2+} ions, but insufficient counting statistics prevented the identification of a similar structure for O^{6+} ions with velocities greater than 500 km/s [Fuselier et al., 1988]. There appear to be no published models applicable to these observations.

We have developed a three fluid model to study the jumps in flow properties across MHD fast and slow shocks

Paper number 90JA02753.
0148-0227/91/90JA-02753$05.00

[Whang et al., 1990, hereafter referred to as paper 1], and the predictions of the model for the case of the coronal slow shock may provide an explanation for the characteristics of minor ions in the solar wind if the physical processes taking place between the downstream side of the coronal slow shock and the place where the in situ observations were made do not significantly change these ion flow characteristics. In this paper we extend the three fluid model to the case of fast shocks. It is well known that there is a resistive, also called first, critical Mach number in classical MHD fast shocks, above which the MHD equations with resistivity alone do not produce a continuous shock profile [Edmiston and Kennel, 1984, and references therein], and the resistive critical Mach number has a meaning even for collisionless shocks [Kennel et al., 1985]. Kennel [1987] recently obtained a new critical Mach number on the basis of the MHD equations including both resistivity and thermal conductivity and showed that resistivity and thermal conductivity can provide convergent stationary point solutions for all but switch-off slow shocks. In contrast to slow shocks, however, there always exist critical Mach numbers for fast shocks. Observations and simulations of fast shock structure indicate that there are distinguishing differences between the magnetic profiles of supercritical and subcritical Mach number shocks [Gosling and Robson, 1985; Greenstadt, 1985; Gosling et al., 1989; Onsager et al., 1990]. As shown later and by paper 1, solutions of jump conditions for three species are shock structure dependent. Thus existence of the critical Mach number for fast shocks suggests that it may be difficult to find a motion pattern for minor ions to cover all the domain in the parameter space of fast Mach number M_f, the plasma β, and shock angle θ_1. The major goal of the present work is to explore, by parameter studies, the extent to which the three-fluid model can be used to describe the ion heating and deceleration, and to identify some physical processes probably taking place within the shock transition layer.

2. Mathematical Formulation

2.1. Rankine-Hugoniot Relations

The jumps in flow properties across a MHD shock in a frame of reference attached to the shock can be described by the classical theory of MHD shocks, which leads to the Rankine-Hugoniot relations. We choose a Cartesian coordinate system: the x axis is normal to the shock surface, pointing in the direction of the mass flow in a shock rest frame of reference, and the tangential component of the magnetic field points in the positive direction of the y axis; thus the xy plane is the plane of coplanarity. We formulate the flow conditions in the de Hoffmann-Teller frame of reference. Thus outside the shock layer, the MHD fluid velocity $\mathbf{U}$ is aligned with the magnetic field $\mathbf{B}$, and the electric field $\mathbf{E}$ and the noncoplanarity component of the magnetic field, B_z, are zero. The jumps in the magnetic field $\mathbf{B}$ and the MHD fluid density ρ, velocity $\mathbf{U}$, and temperature T outside the shock layer can be determined from the flow conditions upstream of the shock by using the MHD conservation equations in the de Hoffmann-Teller frame of reference,

$$[\rho U_x] = 0 \tag{1}$$

$$\rho U_x[\mathbf{U}] + [P + B^2/8\pi]\mathbf{e}_x - B_x[\mathbf{B}]/4\pi = 0 \tag{2}$$

$$[U^2/2 + (\gamma/(\gamma-1))P/\rho] = 0 \tag{3}$$

$$[B_x] = 0 \tag{4}$$

Here γ is the ratio of specific heats for the plasma as a whole, and the pair of square brackets denotes the jump of a physical quantity across the shock,

$$[Q] = Q_2 - Q_1$$

where the subscripts 1 and 2 denote the flow conditions upstream and downstream, respectively, of the shock.

Whang [1987, 1988] showed that the downstream to upstream ratios B_2/B_1, ρ_2/ρ_1, U_{x2}/U_{x1}, and P_2/P_1 are functions of three dimensionless upstream parameters, i.e., the shock Alfven number $A = U_{x1}/(a_1 \cos\theta_1)$, the shock angle θ_1, and the plasma β value (here a is the Alfven speed, and β the ratio of the thermal pressure P_1 to the magnetic pressure $B_1^2/8\pi$). For a fast shock the shock Alfven number on both sides of the shock must be greater than 1, and the magnetic field and the shock angle increase across the fast shock. For a slow shock the shock Alfven number must be less than 1, and the magnetic field and the shock angle decrease across the slow shock.

The shock Alfven number, A, is related to the Mach number M by

$$A^2 = \{(1+\gamma\beta/2) \pm ((1+\gamma\beta/2)^2 - 2\gamma\beta\cos^2\theta_1)^{1/2}\}M^2/(2\cos^2\theta_1) \tag{5}$$

Here the upper (lower) sign is for fast (slow) shocks, and the Mach number in the case of fast (slow) shocks is expressed as M_f (M_s) hereafter. The Mach number is sometimes used in place of the Alfven number as an independent variable to calculate the shock relationships. In the M, β, θ_1 parameter space, fast shock solutions exist in the domain of $M_f > 1$, and slow shock solutions exist in the domain of $M_s > 1$.

It should be noted that the Rankine-Hugoniot relations do not depend on the shock structure, and in the de Hoffmann-Teller frame of reference there is no energy exchange between the electromagnetic fields and the plasma as a whole [Jones and Ellison, 1987]. However, the energy partition among the three species of the plasma depends strongly on variation of the electromagnetic fields and the flow properties of each species through the shock.

2.2. Jump Conditions for Polytropic, Massless Electrons

The one-fluid MHD theories cannot predict the energy partition among electrons, protons, and other ions such as α particles. We will try to use here a three-fluid model with given energy partition on the upstream side of a fast shock and a specified value of the ratio of specific heats for the minor ions to predict the possible energy partition

among the three species on the downstream side of the shock.

It has long been recognized that collisionless shocks do not heat electrons as efficiently as they heat ions [Feldman, 1985 and references therein]. We will assume the electrons to be a polytropic, massless gas and replace the energy equation of electrons by

$$T_{e2}/T_{e1} = \eta_e^{(\gamma_e - 1)} \tag{6}$$

Here the ratio of electron densities downstream to upstream is given by

$$\eta_e = n_{e2}/n_{e1} = \{\eta + (\eta\mu - (\mu - 2)\eta_\alpha)\epsilon\}/(1 + 2\epsilon), \tag{7}$$

where η and η_α denote the ratio of fluid density and α particle density downstream to upstream, respectively, ϵ denotes the upstream density ratio of the minor ions to protons, and μ the mass ratio of minor ions to protons. It follows that $\eta_e = \eta$ if ϵ can be neglected.

The momentum equation for the polytropic, massless electrons thus becomes

$$\int (\mathbf{E} + \mathbf{U}_e \times \mathbf{B}/c)_x dx = -(\gamma_e/(\gamma_e - 1))k[T_e] \tag{8}$$

It will be seen later that the cross-shock electrostatic potential difference $[\phi]$ can be derived from the above equation to be proportional to the electron temperature difference $[T_e]$, i.e., $e[\phi] \propto k[T_e]$. It thus follows that with the polytropic index γ_e given, the cross-shock electrostatic potential difference can be determined if the density ratio η_α for minor ions can be determined.

2.3. Jump Conditions for Minor Ions

As derived in paper 1, the equations for conservation of mass, momentum, and energy for minor ions can be integrated to give

$$[n_\alpha U_{\alpha x}] = 0 \tag{9}$$

$$[n_\alpha m_\alpha U_{\alpha x}^2 + n_\alpha k T_\alpha] = F_\alpha \tag{10}$$

$$[n_\alpha m_\alpha U_{\alpha x} U_{\alpha y}] = G_\alpha \tag{11}$$

and

$$[(U_{\alpha x}^2 + U_{\alpha y}^2)/2 + (\gamma_\alpha/(\gamma_\alpha - 1))kT_\alpha/m_\alpha] = H_\alpha \tag{12}$$

where γ_α is the ratio of specific heats for the minor ions. The cross-shock integrated values F_α and G_α represent the accumulated effects of the Lorentz forces over the shock layer on the momentum flux of minor ions. The integrated value H_α is the spatial integral of the work done by minor ions against the electrostatic field. It follows from the above equations that F_α, G_α, and H_α depend on the shock structure, i.e., the profiles of n_α, $\mathbf{U}_\alpha$, and $\mathbf{U}_e$ as well as $\mathbf{E}$ and $\mathbf{B}$. Therefore, unlike the MHD fluid jump conditions, the jump conditions for minor ions are shock structure dependent. F_α, G_α, and H_α can only be approximately estimated because we do not know the detailed shock structure. Any deviation from the accurate integrated value will affect the accuracy of the solution and even its existence.

Observations of ion distributions at the Earth's bow shock indicate that positive ions are reflected just upstream of the magnetic ramp, then gyrate in the magnetic foot, and their guiding centers drift toward the downstream side of the shock for quasi-perpendicular shocks and backward to the upstream side of the shock for quasi-parallel shocks [Gosling and Robson, 1985], and for sufficiently high Mach numbers, ion reflection is the primary process by which ion energy dissipation is initiated at quasi-parallel, collisionless shocks as well as quasi-perpendicular shocks in space [Gosling et al., 1989; Onsager et al., 1990]. Following paper 1, we use symbol $\mathbf{L}_K^M$ to denote the magnetic Lorentz force on the species $K = e, p$, or α due to perpendicular electric current caused by the sudden change in the magnetic configuration inside the shock and use guiding center theory to estimate the ratios

$$|\mathbf{L}_e^M| : |\mathbf{L}_p^M| : |\mathbf{L}_\alpha^M|$$

Then we obtain the following spatial integrals:

$$F_\alpha = -Z_\alpha < \frac{n_\alpha}{n_e} > [n_e k T_e] - < \Gamma_\alpha > \frac{[B_y^2]}{8\pi} \tag{13}$$

$$G_\alpha = -Z_\alpha < \frac{n_\alpha B_y}{n_e B_x} > [n_e k T_e] + < \Gamma_\alpha > \frac{B_x [B_y]}{4\pi} \tag{14}$$

$$H_\alpha = -\frac{Z_\alpha}{m_\alpha} < \frac{B^2}{B_x^2} > \frac{\gamma_e}{\gamma_e - 1} k[T_e] \tag{15}$$

where

$$\Gamma_\alpha = \frac{P_{\|\alpha} - P_{\perp\alpha}}{(P_{\|p} - P_{\perp p}) + (P_{\|\alpha} - P_{\perp\alpha})} \tag{16}$$

For the convenience of computations, we can write

$$\gamma_\alpha = \frac{n_\alpha T_\alpha}{\chi n_p T_p + n_\alpha T_\alpha}$$

Here coefficient $\chi = (a_p - 1)(a_\alpha - 1)/((a_\alpha - 1)(a_p + 2))$ and $a_K = (P_\|/P_\perp)_K$, $K = \alpha$ or p. Observations show that the α particle thermal anisotropy is generally slightly, but perhaps not significantly, lower than that for protons [Marsch et al., 1982 and references therein]. In the numerical computation we assume that the distribution functions of the solar wind minor ions and protons have similar asymmetries with respect to the magnetic field. Thus we have $\chi \simeq 1$. The assumption may appear to be a strong one. The numerical calculations show that no significant changes can be found in the final solutions if a_α differs from a_p by 20%, as shown in paper 1. The pair of angle brackets $< Q >$ in expressions (13)–(15), according to the extension of the mean value theorem for integrals, can be expressed by

$$< Q > = \frac{\int Q R dx}{\int R dx}$$

with the condition of $R \geq 0$. Here R represents $d(n_e T_e)/dx$, dB^2/dx, or dT_e/dx in the transition region. In numerical calculation it will be approximately replaced by $< Q > \simeq \omega Q_1 + (1 - \omega) Q_2$, and here ω is a fractional factor between 0 and 1.

Expression (15) indicates that the term on the right-hand side of the energy equation represents an energy sink. The minor ions do work as they move against the electro-

static field inside the shock layer. The part of the energy loss of the minor ions will be transferred to electrons.

2.4. Proton Properties on the Downstream Side of the Shock

Once we have solutions for the MHD fluid, electron gas, and minor ion gas, the proton properties on the downstream side of the fast shock can be directly calculated as follows:

$$\eta_p = \eta + (\eta - \eta_\alpha)\mu\epsilon \tag{17}$$

$$\mathbf{U}_{p2} = \mathbf{U}_2 - 4\epsilon(\eta_\alpha/\eta_p)(\mathbf{U}_2 - \mathbf{U}_{\alpha 2}) \tag{18}$$

$$T_{p2} = (P_2 - n_{e2}kT_{e2} - n_{\alpha 2}kT_{\alpha 2})/(kn_{p2}) - (m_p n_{p2} W_p^2 + m_\alpha n_{\alpha 2} W_\alpha^2)/(3kn_{p2}) \tag{19}$$

where W_p and W_α are the magnitudes of the diffusion velocities of protons and minor ions. Equation (17) indicates

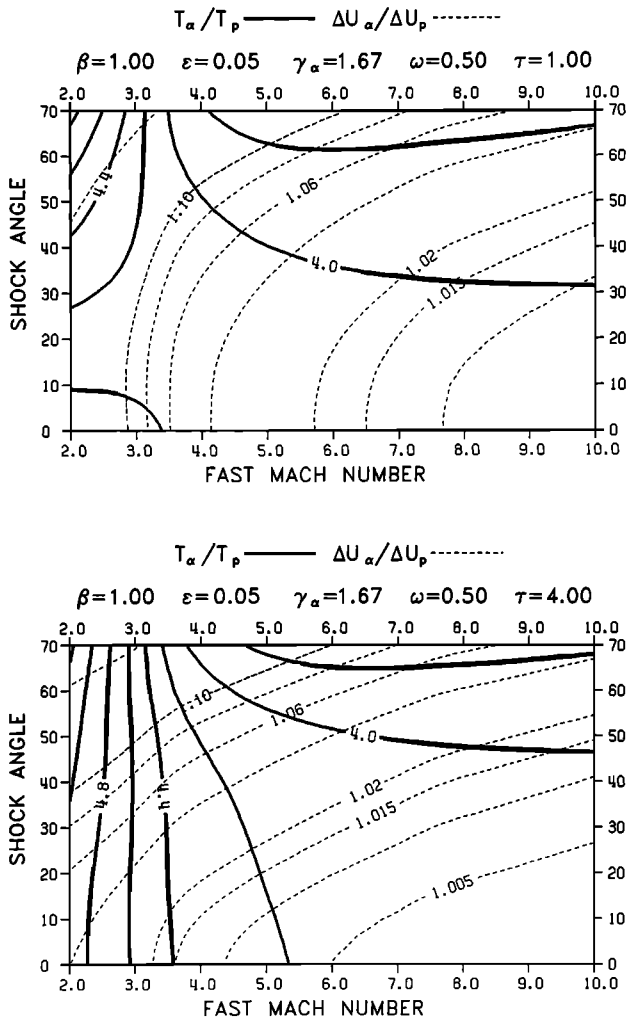

Fig. 1, The solid curves denote the constant contours for $T_{\alpha 2}/T_{p2}$, and the dashed curves for $\Delta U_\alpha/\Delta U_p$. The upper panel and the lower panel are, respectively, for the case of $\tau = 1.0$ and 4.0, i.e., for the case of the collisional solar wind and the collisionless solar wind being on the upstream side of the shocks.

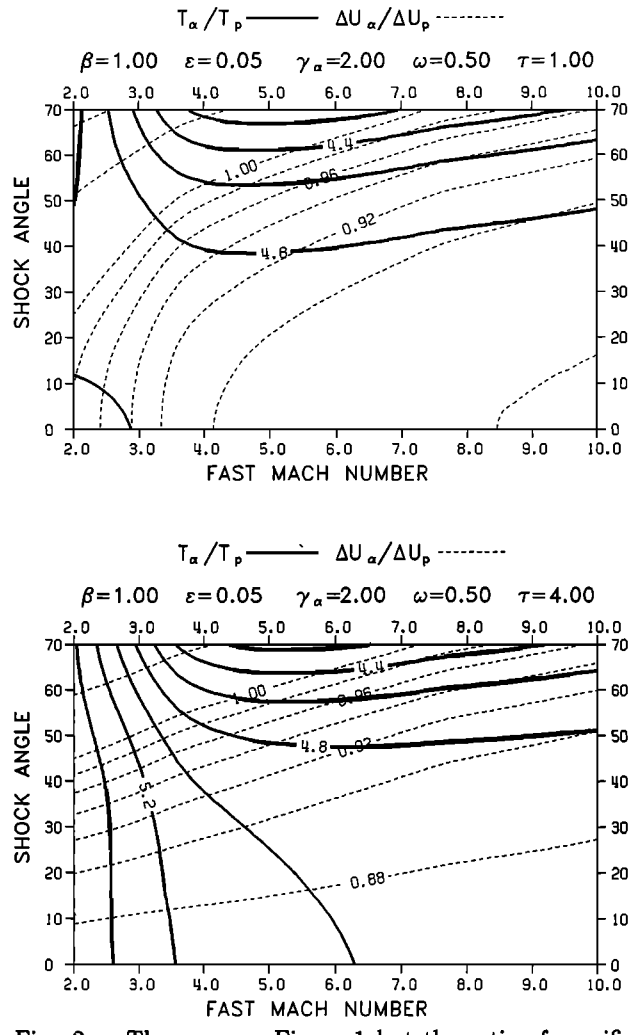

Fig. 2, The same as Figure 1 but the ratio of specific heats for α particles is $\gamma_\alpha = 2.0$.

that the density ratio of protons downstream to upstream, η_p, is less than η if η_α is greater than η. Because of the larger mass and thus the smaller acoustic speed of the minor ion, η_α appears to be greater than η and, in general, η_p. With the condition of identical upstream temperature for all three kinds of species, the ratio $U_{\alpha x2}/U_{px2}$ must, in general, be less than 1 under the assumption of $U_{\alpha x1}$ equal to U_{px1} and $\gamma_\alpha = \gamma_p = \gamma$. Only in the case of $\epsilon \simeq 0$, which applies to the minor ions other than α particles, $\eta_p \simeq \eta$ and $\mathbf{U}_{p2} \simeq \mathbf{U}_2$.

3. Computational Scheme

3.1. Energy Partition on the Upstream Side of the Shock

Section 2 provides a theoretical formulation for the jumps in flow properties of electrons, minor ions, and protons across the fast shocks. In order to carry out numerical computations, we need to give the flow conditions on the upstream side of the shock. We assume that all kinds of species have the same velocity there, i.e.,

$$\mathbf{U}_{\alpha 1} = \mathbf{U}_{p1} = \mathbf{U}_{e1} \tag{20}$$

However, the different species usually have different gas temperatures. In the numerical computation we will assume $T_{e1} = T_{p1} = T_1$. For minor ions we will introduce a parameter $\tau = T_{\alpha 1}/T_{p1}$ and try the cases of (1) $\tau = m_\alpha/m_p$ for collisionless upstream flow and (2) $\tau = 1$ for collisional upstream flow. In addition, we will try the cases of (1) $\epsilon = 0.05$ for α particles and (2) $\epsilon \simeq 0$ for other minor ions.

3.2. Numerical Values of γ, γ_α, and γ_e

The energy equations, both for MHD fluid and for minor ions, include a parameter, the ratio of the specific heats, which relates to the number of degrees of freedom. The literature does not provide much theoretical guidance as to the choice of values for these quantities. Observational evidence for plasma to have 2 degrees of freedom lies in the magnitude of the standoff distance of the bow shock from the magnetopause [Fairfield, 1971; Zhuang and Russell, 1981], which agrees best with a theoretical calculation using a ratio of specific heats γ of 2. On the other hand, terrestrial laminar shocks seem to be best approximated with a γ of 5/3 [Russell et al., 1982]. To test whether the solar wind plasma is better approximated as having 2 or 3 degrees of freedom, or to determine if the ratio of specific heats γ should be 5/3 or 2, Russell et al. [1983] have analyzed ISEE three-dimensional plasma data across five interplanetary shocks, each observed with four spacecraft. Their inference is that [Russell et al., p. 9945, 1983] "$\gamma = 5/3$ is appropriate for MHD calculations, but if one is using a gas dynamic model to give the shock position, one should use a γ of 2." On the other hand, Leroy et al. [1982] carried out a simulation of perpendicular shock structure assuming that the ions evolve two-dimensionally in velocity space, while the electrons behave three-dimensionally. The results of the simulation agree very well with observations of quasi-perpendicular shock structure.

In the numerical computation for solution of the MHD fluid we use a γ of 5/3. In the solution of minor ion jump conditions we will calculate with $\gamma_\alpha = 5/3$ and 2 and compare the results with observations to see whether the solar wind minor ions are better approximated as having 2 or 3 degrees of freedom.

The effective polytropic index for electrons γ_e is inferred from observations to be between 5/3 and 3 [Feldman, 1985; Scudder et al., 1986; Thomsen et al., 1987; Schwartz et al., 1988]. We do not know, however, how the effective polytropic index changes quantitatively as the

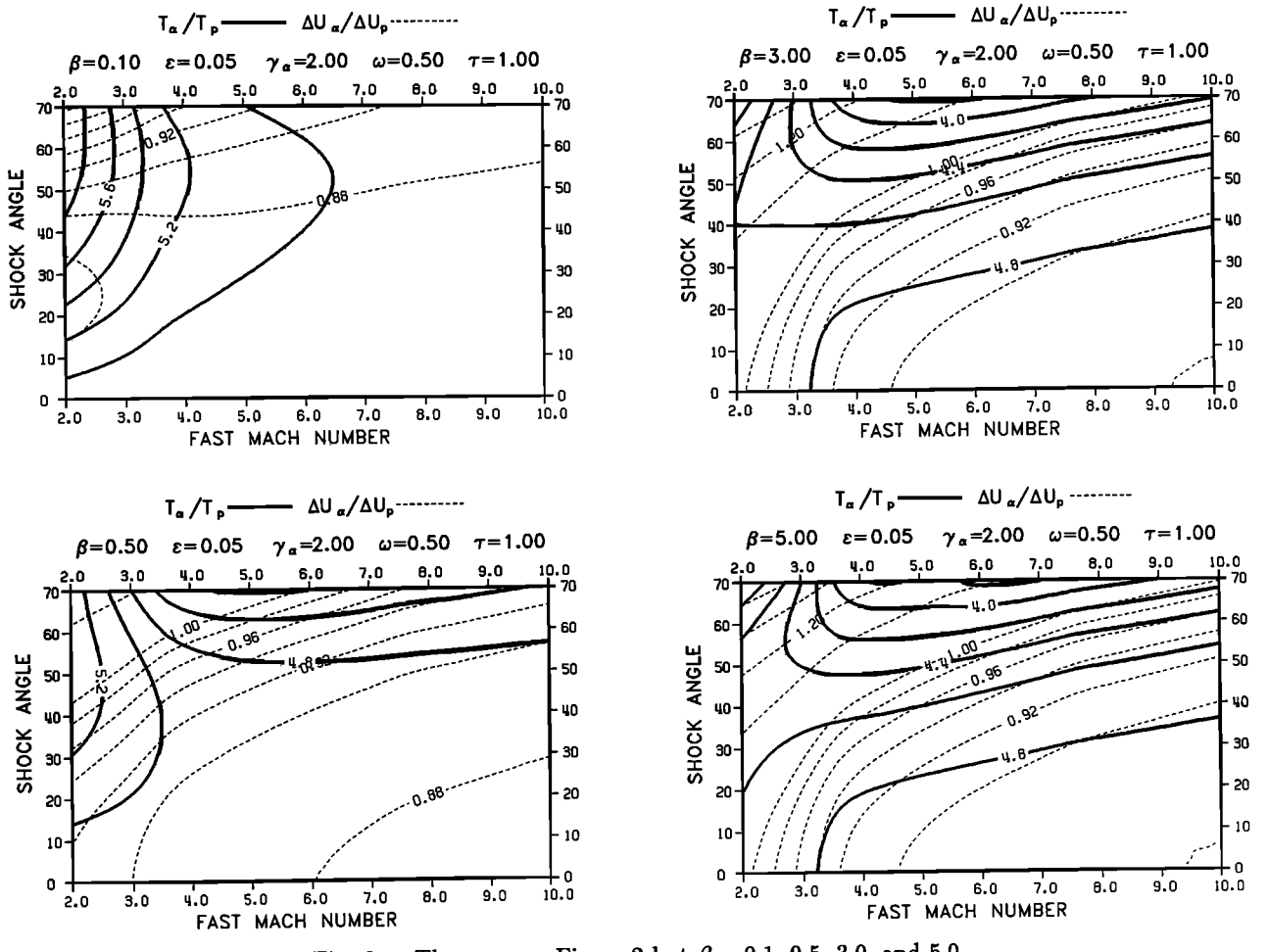

Fig. 3, The same as Figure 2 but $\beta = 0.1$, 0.5, 3.0, and 5.0.

Mach number increases. On the other hand, the "temperature determination" of the cross-shock electrostatic potential difference probably underestimates the potential somewhat, as pointed out by Schwartz et al. If the effective polytropic index were replaced by 5/3, the value of estimated potential difference would be increased by a factor of ≤ 1.7, which shows rough quantitative agreement with the "edge determination" of the potential difference [Schwartz et al., 1988]. Thus computations carried out in this work use only $\gamma_e = 5/3$.

3.3. Computational Scheme

We calculate the flow conditions downstream of the fast shocks, with a particular interest in the two ratios $T_{\alpha 2}/T_{p2}$ and $\Delta U_\alpha/\Delta U_p$. Here $\Delta U_K = |\mathbf{U}_{K2} - \mathbf{U}_{K1}|$, $K = \alpha$, p. These two ratios are independent of the frame of reference. For a given combination of the plasma β value, the shock angle θ_1, and the fast shock Mach number M_f (or the shock Alfven number A), we first calculate the ratios B_2/B_1, ρ_2/ρ_1, U_{x2}/U_{x1}, U_{y2}/U_{y1}, T_2/T_1, and θ_2 using the simple direct method of Whang [1987] for the MHD jump conditions. Then we calculate the flow conditions of minor ions for the ratios $n_{\alpha 2}/n_{\alpha 1}$, $U_{\alpha x2}/U_{\alpha x1}$, $U_{\alpha y2}/U_{\alpha y1}$, and $T_{\alpha 2}/T_{\alpha 1}$ across the shock layer following the method developed in section 2.3 for a set of γ_α and τ. The third step is to calculate the flow conditions of protons using formulas developed in section 2.4. The solutions can be organized as functions of three dimensionless parameters: β, θ_1, plus A or M_f with the γ_α and τ given.

3.4. Iteration

Because the calculated downstream properties for both electrons and protons depend on the downstream properties for α particles, and vice versa, we use an iteration procedure to obtain the self-consistent solutions for all three species. The initial values used in the iteration are $T_{\alpha 2}/T_{p2} = m_\alpha/m_p$ and those corresponding to the case of $\epsilon \simeq 0$; when $\eta_e = \eta_p = \eta$ as shown by expressions (12) and (17), implying that the reaction of the minor ions to the major components of the MHD fluid can be neglected. Since we do not know the detailed structure of the flow and field inside the shock layer, we have to use an approximate method to estimate those weighted average values of physical properties which appear in equations (13), (14), and (15).

4. Results

4.1. Results for α Particles

The shock relations formulated in the de Hoffmann-Teller frame of reference have a singularity at $\theta_1 = 90°$. The iteration scheme also becomes difficult to converge for nearly perpendicular shocks. We carry out numerical solution for $0° \leq \theta_1 \leq 70°$ and $2.0 \leq M_f \leq 10.0$. For a given combination of β, γ_α, and τ, we can construct constant contour plots for $T_{\alpha 2}/T_{p2}$ and $\Delta U_\alpha/\Delta U_p$ on the M_f, θ_1 plane as shown in Figures 1, 2, and 3 for α particles. The solid curves represent the constant contours for $T_{\alpha 2}/T_{p2}$, and the dashed curves those for $\Delta U_\alpha/\Delta U_p$. The two panels in Figure 1 show that the variation of τ ($\tau = 1.0$ for the collisional solar wind and $\tau = 4$ for the collisionless wind) produces changes for $T_{\alpha 2}/T_{p2}$ and $\Delta U_\alpha/\Delta U_p$, especially in the domain of low Mach number $M_f < 4.0$. In general, $T_{\alpha 2}/T_{p2}$ increases and $\Delta U_\alpha/\Delta U_p$ decreases as τ increases. It is seen from Figure 1 that $T_{\alpha 2}/T_{p2}$ is close to or greater than the mass ratio of α particle to proton, and $\Delta U_\alpha/\Delta U_p$ is always greater than 1.0. The two panels in Figure 2 display results for $\tau = 1$ and 4 with $\gamma_\alpha = 2.0$, which show the significant effects of the ratio of specific heats of minor ions on both the temperature ratio and the velocity change ratio. Comparing Figure 2 with Figure 1, we see that as γ_α increases, the temperature ratio increases, the velocity change ratio decreases, and that $\Delta U_\alpha/\Delta U_p$ less than 1.0 occurs in most of M_f, θ_1 space for supercritical Mach number shocks. It suggests that for supercritical Mach number shocks the cross-shock deceleration for minor ions is less than for protons, which agrees with observations.

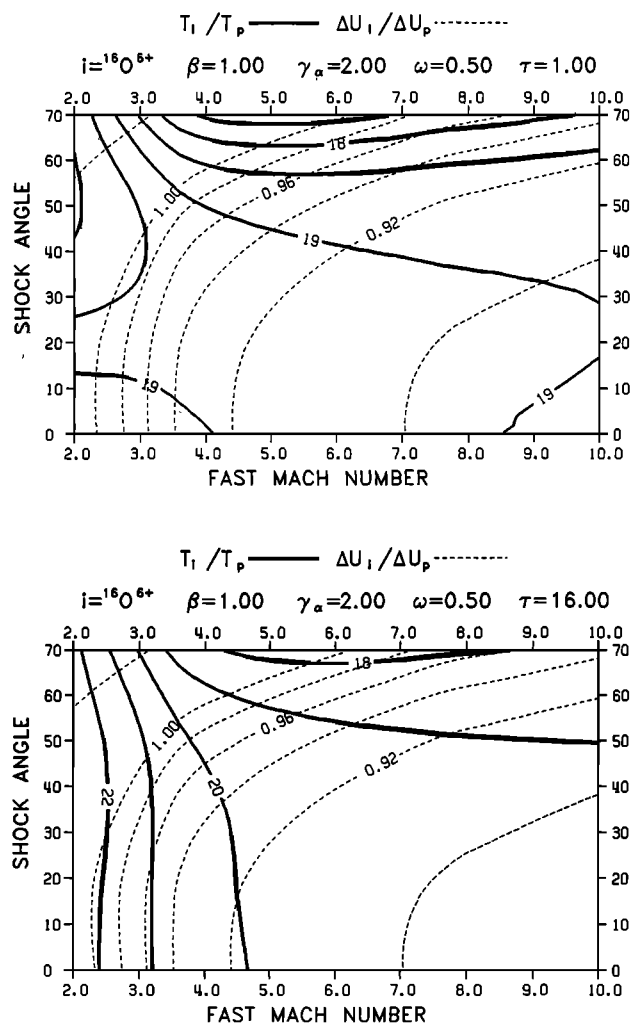

Fig. 4, The three-fluid model is used to calculate the jump conditions for other minor ions. The solid curves denote T_{i2}/T_2, and the dashed curves $\Delta U_i/\Delta U$; here $i = {}^{16}O^{6+}$. The upper panel is for $\tau = 1$ and the lower panel for $\tau = 4$ with $\gamma_i = 2$ and $\beta = 1.0$.

Four contour plots with $\beta = 0.1$, 0.5, 3, and 5 are shown in Figure 3. The plasma β value has a strong effect on the solution of $T_{\alpha 2}/T_{p2}$ and $\Delta U_\alpha/\Delta U_p$, and no solution exists for $M_f < 2$.

The observations of effects on minor ions across a fast shock show that across most of Earth's bow shock and strong interplanetary shocks these ions have temperatures higher than those of protons by up to 5–7 times, and the cross-shock change of minor ion velocity is less than that of protons. The model prediction with $\gamma_\alpha = 2$ agrees with the observations fairly well, suggesting that the heating of minor ions probably involves 2 degrees of freedom.

4.2. Results for Other Minor Ions

The three-fluid model can be used to calculate the conditions of other minor ions across a fast shock. In this case the MHD fluid consists of electrons e, protons p, and a species of minor ions i (e.g., $^{16}O^{6+}$, $^{28}Si^{8+}$, $^{56}Fe^{16+}$). We can assume that $n_i \ll n_p$. Under this assumption, we can infer from expressions (12), (17), and (18) that $n_p \simeq n_e$ and $\mathbf{U}_p \simeq \mathbf{U}$ in the computation. Figures 4–6 show the contour plots for the ratio of minor ion velocity change ΔU_i to fluid velocity change ΔU and the ratio of minor ion temperature T_{i2} to fluid temperature T_2, for $^{16}O^{6+}$, $^{28}Si^{8+}$ and $^{56}Fe^{16+}$, respectively, at two τ values. Once again these figures show that the temperature ratio roughly proportional to ion mass is the most important dynamic effect of a shock wave on minor ions. A careful examination of Figures 5 and 6 reveals a striking result that the constant contours for ΔU_i and T_{i2}/m_i are almost identical in these plots, the same as shown in the case of slow shocks. Identically, the characteristic can be explained by the similarity relationship derived in paper 1.

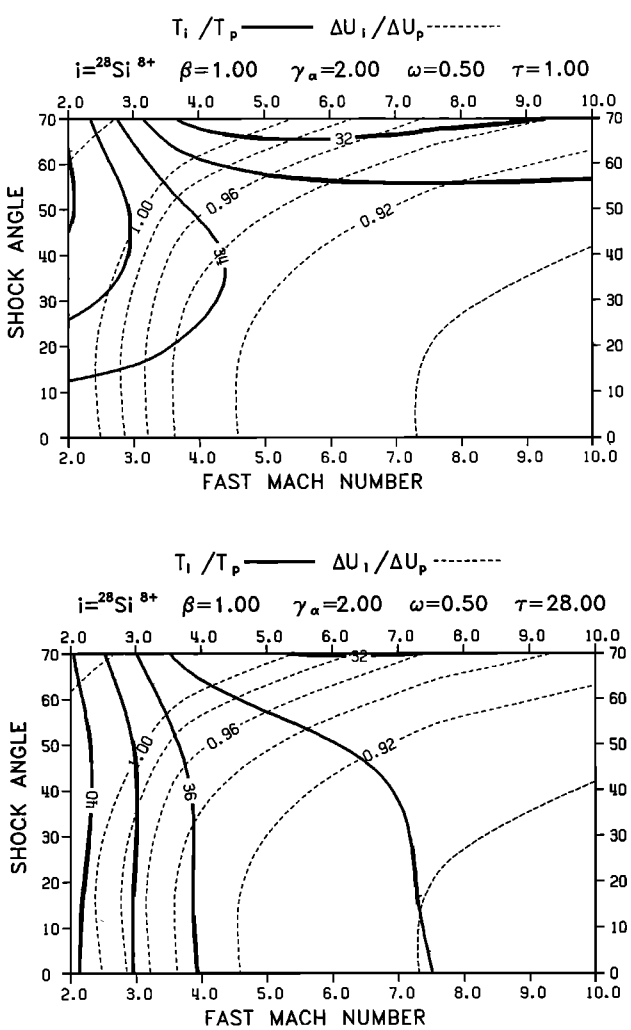

Fig. 5, The same as Figure 4 but $i = {}^{28}Si^{8+}$.

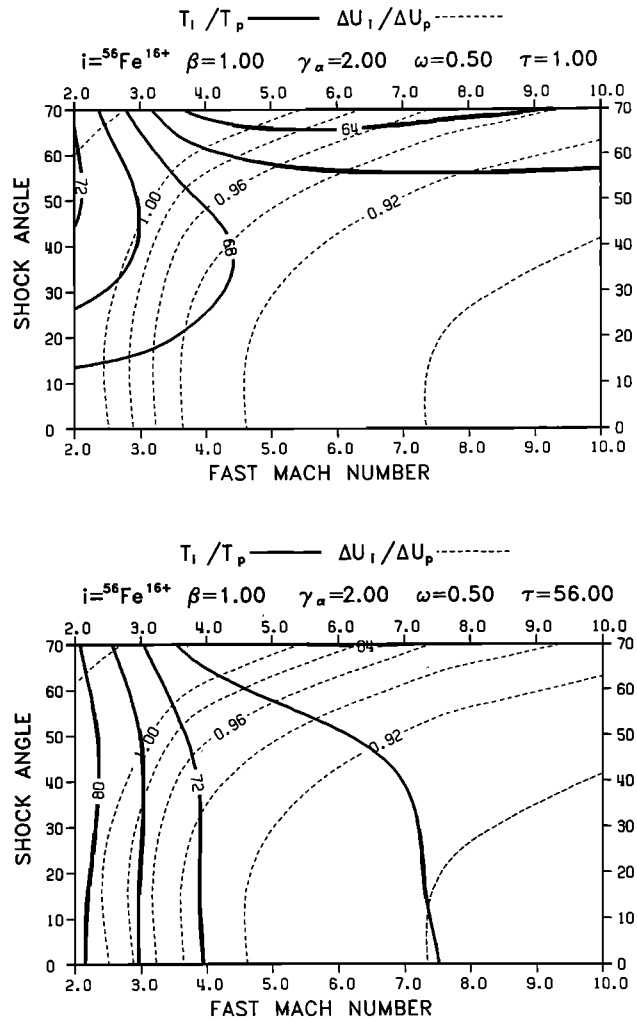

Fig. 6, The same as Figure 4 but $i = {}^{56}Fe^{16+}$.

5. Conclusions and Discussion

Comparison of predictions of the three-fluid model to observations of effects on minor ions across a fast shock indicates that the three-fluid model used here can explain cross-shock minor ion heating significantly greater than that of protons. If we assume $\gamma_\alpha = 2$, the model predictions of both $T_{\alpha 2}/T_{p2}$ and $\Delta U_\alpha/\Delta U_p$ agree fairly well with observations. This suggests that the heating of the minor ions probably involves 2 degrees of freedom. Further confirmation of these predictions might be obtained at the bow shock.

The energy partition among the three kinds of species making up the plasma considered as an MHD fluid is a shock structure dependent problem. The existence of the critical Mach number for fast collisionless shocks and the differences shown in the supercritical and subcritical Mach number shock transition regions suggest that it may be unreasonable to expect a single model to cover the whole domain of M_f, θ_1 space, including both supercritical and subcritical, and both quasi-perpendicular and quasi-parallel shocks. Observations [Gosling et al., 1988, 1989; Mellott, 1985] suggest that the ion motion within the low Mach number shock transition region is largely restricted in the coplanarity plane. The guiding center velocity used in estimating the electromagnetic forces on the minor ions, however, is not restricted to the coplanarity plane. That might be why the model predictions presented above can only agree with observations for supercritical Mach number shocks. Therefore, in order to predict the flow conditions on the downstream side of low Mach number shocks, the ion velocity parallel to the coplanarity plane appears to be a reasonable assumption.

Acknowledgments. The work at the Catholic University of America was supported by National Science Foundation under NSF grant ATM-9012366. X. Zhao expresses his thanks for the hospitality of Dr. Y. C. Whang while he was a visitor at the Catholic University of America.

The Editor thanks S. A. Fuselier and another referee for their assistance in evaluating this paper.

References

Edmiston, J. P., and C. F. Kennel, A parametric survey of the first critical Mach number for a fast MHD shock, *J. Plasma Phys., 32*, 429–439, 1984.

Fairfield, D. H., Average and unusual locations of the Earth's magnetopause and bow shock, *J. Geophys. Res., 76*, 6700–6716, 1971.

Feldman, W. C., Electron velocity distributions near collisionless shocks, in *Collisionless Shocks in the Heliosphere: Reviews of Current Research, Geophys. Monogr. Ser., vol. 35*, edited by B. T. Tsurutani and R. G. Stone, pp. 195–205, AGU, Washington, D. C., 1985.

Fuselier, S. A., E. G. Shelley, and D. M. Klumpar, AMPTE/CCE observations of shell-like He^{2+} and O^{6+} distributions in the magnetosheath, *Geophys. Res. Lett., 15*, 1333–1336, 1988.

Gosling, J. T., and A. E. Robson, Ion reflection, gyration, and dissipation at supercritical shocks, in *Collisionless Shocks in the Heliosphere:Reviews of Current Research, Geophys. Monogr. Ser., vol. 35*, edited by B. T. Tsurutani and R. G. Stone, pp. 141–152, AGU, Washington, D. C., 1985.

Gosling, J. T., D. Winske, and M. F. Thomsen, Noncoplanar magnetic fields at collisionless shocks: A test of new approach, *J. Geophys. Res., 93*, 2735–2740, 1988.

Gosling, J. T., M. F. Thomsen, S. J. Bame, and C. T. Russell, Ion reflection and downstream thermalization at the quasi-parallel bow shock, *J. Geophys. Res., 94*, 10,027–10,038, 1989.

Greenstadt, E. W., Oblique, parallel, and quasi-parallel morphology of collisionless shocks, in *Collisionless Shocks in the Heliosphere:Reviews of Current Research, Geophys. Monogr. Ser., vol. 35*, edited by B. T. Tsurutani and R. G. Stone, pp. 169–184, AGU, Washington, D. C., 1985.

Jones, F. C., and D. C. Ellison, Noncoplanar magnetic fields, shock potentials, and ion deflection, *J. Geophys. Res., 92*, 11,205–11,207, 1987.

Kennel, C. F., J. P. Edmision, and T. Hada, A quater century of collisionless shock research, in *Collisionless Shocks in the Heliosphere: A Tutorial Reviews, Geophys. Monogr. Ser., vol. 34*, edited by B. T. Tsurutani and R. G. Stone, pp. 1–36, AGU, Washington, D. C., 1985.

Kennel, C. F., Critical Mach numbers in classical magnetohydrodynamics, *J. Geophys. Res., 92*, 13,427–13,437, 1987.

Leroy, M. M., D. Winske, C. C. Goodrich, C. S. Wu, and K. Papadopoulos, The structure of perpendicular bow shock, *J. Geophys. Res., 87*, 5081–5094, 1982.

Marsch, E., K.-H. Muhlhauser, H. Rosenbauer, R. Schwenn, and F. M. Neubauer, Solar wind helium ions: Observations of the Helios solar probes between 0.3 and 1 AU, *J. Geophys. Res., 87*, 35–51, 1982.

Mellott, M. M., Subcritical collisionless shock waves, in *Collisionless Shocks in the Heliosphere:Reviews of Current Research, Geophys. Monogr. Ser., vol. 35*, edited by B. T. Tsurutani and R. G. Stone, pp. 131–140, AGU, Washington, D. C., 1985.

Neugebauer, M., Initial deceleration of solar wind positive ions in the Earth's bow shock, *J. Geophys. Res., 75*, 717–733, 1970.

Neugebauer, M., Observations of solar wind helium, *Cosmic Phys., 7*, 131–199, 1981.

Ogilvie, K. W., P. Bochsler, J. Geiss, and M. A. Coplan, Observations of the velocity distribution of solar wind ions, *J. Geophys. Res., 85*, 6069–6074, 1980.

Ogilvie, K. W., M. A. Coplan, and R. D. Zwickl, Helium, hydrogen, and oxygen velocities observed on ISEE 3, *J. Geophys. Res., 87*, 7363–7369, 1982.

Onsager, T. G., M. F. Thomsen, J. T. Gosling, S. J. Bame, and C. T. Russell, Survey of coherent ion reflection at the quasi-parallel bow shock, *J. Geophys. Res., 95*, 2261–2271, 1990.

Peterson, W. K., E. G. Shelley, R. D. Sharp, R. G. Johnson, J. Geiss, and H. Rosenbauer, H^+ and He^{++} in the dawnside magnetosheath, *Geophys. Res. Lett., 6*, 667–670, 1979.

Russell, C. T., M. M. Hoppe, W. A. Livesey, J. T. Gosling, and S. T. Bame, ISEE-1 and -2 observations of laminar bow shocks: Velocity and thickness, *Geophys. Res. Lett., 9*, 1171–1174, 1982.

Russell, C. T., J. T. Gosling, R. D. Zwickl, and E. J. Smith, Multiple spacecraft observations of interplan-

etary shocks: ISEE three-dimensional plasma measurements, *J. Geophys. Res.*, *88*, 9941–9947, 1983.

Schmidt, W. K., H. Rosenbauer, E. G. Shelley, and J. Geiss, On temperature and speed of He^{++} and O^{6+} ions in the solar wind, *Geophys. Res. Lett.*, *7*, 697–700, 1980.

Schwartz, S. J., M. F. Thomsen, S. J. Bame, and J. Stansberry, Electron heating and the potential jump across fast mode shocks, *J. Geophys. Res.*, *93*, 12,923–12,931, 1988.

Scudder, J. D., A. Mangeney, C. Lacombe, C. C. Harvey, T. L. Aggson, R. R. Anderson, J. T. Gosling, G. Paschmann, and C. T. Russell, The resolved layer of a collisionless, high β, supercritical, quasi-perpendicular shock wave, 1, Rankine-Hugoniot geometry, currents, and stationarity, *J. Geophys. Res.*, *91*, 11,019–11,052, 1986.

Thomsen, M. F., M. M. Mellott, J. A. Stansberry, S. J. Bame, J. T. Gosling, and C. T. Russell, Strong electron heating at the Earth's bow shock, *J. Geophys. Res.*, *92*, 10,119–10,124, 1987.

Whang, Y. C., Slow shocks and their transition to fast shocks in the inner solar wind, *J. Geophys. Res.*, *92*, 4349–4356, 1987.

Whang, Y. C., Evolution of interplanetary slow shocks, *J. Geophys. Res.*, *93*, 251–255, 1988.

Whang, Y. C., X. Zhao, and K. W. Ogilvie, Heating of minor ions by the coronal slow shock, *J. Geophys. Res.*, *95*, 18,781–18,790, 1990.

Zastenker, G. N., and N. L. Borodkova, Interplanetary shock waves in April—May 1981, *Kosm. Issled.*, *22*, 87–96, 1984. (*Cosmic Res.*, Engl. Transl., *22*, 77–85, 1984.)

Zastenker, G., O. Vaisberg, Z. Nemechek, Ya. Shafrankova, I. Kozak, and M. Shevchenko, Physical peculiarities of fine structure of the collisionless shock front by direct space measurements, in *Proceedings of the International Conference on Collisionless Shocks*, edited by K. Szego, Press of the Hungarian Academy of Sciences, pp. 62–69, Budapest, 1987.

Zhuang, H.-C., and C. T. Russell, An analytic treatment of the structure of the bow shock and magnetosheath, *J. Geophys. Res.*, *86*, 2191–2205, 1981.

K. W. Ogilvie, NASA Goddard Space Flight Center, Code 692, Greenbelt, MD 20771,

Y. C. Whang, Department of Mechanical Engineering, Catholic University of America, Washington, DC 20064.

X. Zhao, CSSA ERL 329, Stanford University, Stanford, Stanford, CA 94305.

(Received July 19, 1990;
accepted September 17, 1990.)